Data-driven IQC-Based Robust Control Design for Hybrid Micro-disturbance Isolation Platform

Vaibhav Gupta[1], Elias Klauser[2] and Alireza Karimi[1]

***Abstract*— A novel approach for robust controller synthesis, which models uncertainty as an elliptical set, is proposed in the paper. Given a set of frequency response functions of linear time-invariant (LTI) multiple-input multiple-output (MIMO) systems, the approach determines the 'best' linear nominal model and the corresponding elliptical uncertainty set, which is consistent with the data. Using a novel split representation, the uncertainty set is represented as an equivalent integral quadratic constraint (IQC). Finally, this IQC is integrated into a data-driven frequency-domain controller synthesis method using convex optimisation. The proposed method is used to design a controller, which is robust against mechanical uncertainties for a hybrid micro-disturbance isolation platform for space applications. The experimental results show that the proposed method provides a less conservative uncertainty set and improves attenuation performance compared to classical methods that use disk uncertainty.**

I. Introduction

Novel high-precision optical instruments designed for Earth observation missions demand an exceptionally high pointing accuracy. These line-of-sight stability requirements constrain the admissible level of mechanical vibration that can occur onboard a spacecraft. Micro-disturbances are caused by primary satellite systems such as reaction wheels, thrusters, cryocoolers, or solar array drive mechanisms, and can potentially lead to a significant performance degradation of the sensitive payloads.

A hybrid active-passive micro-disturbance mitigation system was developed by Airbus in collaboration with the European Space Agency (ESA) [1]. The platform was designed to isolate the spacecraft from perturbations of a reaction wheel. Based on this system, a methodology for uncertainty modelling, robust control design, and the analysis of such systems considering worst-case scenarios for typical satellite observation missions were developed [2]. The study presents a new disturbance model for the multi-harmonic perturbation spectrum generated by rotating reaction wheels. This model can be used for both controller synthesis and worst-case analysis offering new possibilities for simulating the image distortions induced by such disturbances.

Following the promising results achieved by [2], a hybrid active-passive micro-disturbance isolation platform, aimed at mitigating micro-disturbances and isolating the sensitive optical payload from external disturbances, was developed at CSEM. The objective is to study in a more general context the stabilisation of sensitive active payloads from multiple unknown external perturbations. The modular platform consists of an adjustable number of passive dampers, a set of proof mass actuators (PMA) creating a 6 degree of freedom (DoF) force tensor, and a payload interface allowing to accommodate various types of sensitive instruments. The platform utilises the accelerometer measurements in close proximity to the payload to actively reject disturbances from the satellite body. An image of the system is shown in Figure 1. All experimental tests with the platform are carried out at the Microvibration Characterisation Facility at CSEM in Neuchâtel, Switzerland [3].

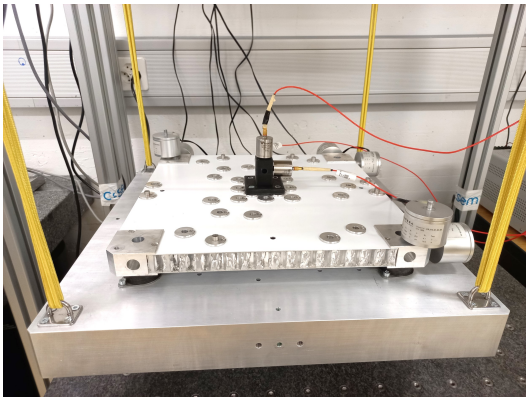

Fig. 1: Hybrid micro-disturbance isolation platform developed at CSEM, Switzerland

Due to the modular nature of the setup and the payload, a parametric plant model is difficult to identify. Furthermore, the passive stage of the setup is highly sensitive to mechanical uncertainties, such as the applied screw torque and other system properties. Hence a robust data-driven control design technique, that can directly minimise a control criterion based on the measured input-output data, is particularly advantageous. A common requirement for such systems is rejecting perturbations within specific frequency ranges. Hence, data-driven methods that utilise frequency-domain data and convex optimisation for computing robust controllers are pertinent here.

Use of frequency-domain data for fixed-structure $\mathcal{H}_\infty$ controller synthesis generally leads to a non-convex optimisation, which can be solved using non-smooth optimisation techniques as proposed in [4]. Several solutions using a convex approximation have also been proposed in the lit-

*This work is funded by Swiss National Science Foundation under grant no. 200021-204962 and ESA Contract No. 4000133258/20/NL/MH/hm.

[1]V. Gupta and A. Karimi are with Laboratoire d'Automatique, École Polytechnique Fédérale de Lausanne, CH-1015 Lausanne, Switzerland vaibhav.gupta, alireza.karimi@epfl.ch

[2]E. Klauser is with CSEM SA, Rue Jaquet-Droz 1, CH-2002 Neuchâtel, Switzerland elias.klauser@csem.ch

erature. For instance, in [5] and [6], computation of SISO-PID controllers is represented as a convex optimisation using constraint linearisation. In [7], MIMO-PID controllers are computed using a convex-concave optimisation by linearising the quadratic matrix inequalities. Using similar linearisation, linearly parameterised MIMO controllers can also be designed [8]. In [9], a frequency-based data-driven control design methodology with $\mathcal{H}_\infty$ control objective based on coprime factorisation of the controller is proposed, and extended to systems with sector nonlinearity in [10]. In [11], this method is employed for linear parameter varying controller design and used for the control moment gyroscopes (CMG) in [12]. Finally, a fixed-structure data-driven controller design method for MIMO systems with mixed $\mathcal{H}_2/\mathcal{H}_\infty$ sensitivity performance is proposed in [13].

The aim of the discussed robust control design methods is to optimise the performance of a nominal model, while also being robust to the uncertainties in the model. This robustness introduces conservatism in the controller. Therefore, it is crucial to identify the 'best' nominal model and the smallest uncertainty set. Classically, one of the measurements or their average is chosen as the nominal system model and the smallest disk that covers all realisations as the uncertainty set [14]. Hindi et al. [15] proposed a technique for the simultaneous identification of the nominal model and the disk uncertainty set, which reduces the radius of the uncertainty set compared to classical methods. More recently, simultaneous identification of the nominal model and the elliptical uncertainty set was presented for SISO systems in [16] and integrated with the controller design method of [13] using the IQC framework of [17].

This paper provides a method for the simultaneous identification of the best linear nominal model and the optimal elliptical uncertainty set of MIMO systems with elementwise uncertainty. First, the notations and a brief introduction to IQC and data-driven controller design using frequency-domain data are given (Section II). Then, the elliptical uncertainty set is represented in the form of a non-parametric IQC, which is then integrated into the data-driven robust controller design reducing conservatism compared to the existing methods (Section III). Finally, the proposed method is used to design a controller for the hybrid micro-disturbance isolation platform which is robust with respect to mechanical uncertainties (Section IV). The contribution of this paper covers that of [16] for SISO systems as a special case.

II. Preliminaries

Notations

The set of real rational stable transfer functions with bounded infinity norm is denoted by $\mathcal{RH}_\infty$. $M \succ (\succeq)\, N$ indicates that $M-N$ is a positive (semi-) definite matrix and $M \prec (\preceq)\, N$ indicates $M-N$ is negative (semi-) definite. The zero and identity matrices of appropriate size are denoted $\mathbf{0}$ and I respectively. The transpose of a matrix M is denoted by M^T and its conjugate transpose by M^*. Right inverse of M is denoted as $M^{\mathsf{R}} = M^*(MM^*)^{-1}$, and its left inverse is denoted as $M^{\mathsf{L}} := (M^*M)^{-1}M^*$. Kronecker product of two matrices M and N is denoted using $M \otimes N$. $\mathrm{diag}(M_1, \cdots, M_n)$ is a block diagonal matrix with $M_1, \cdots, M_n$ lying along the diagonal. For continuous-time systems $\Omega := \mathbb{R}$ and for discrete-time systems $\Omega := [-\pi/T_s, \pi/T_s)$, where T_s is the sampling time. $G(j\omega)$ will be used to denote the frequency response of G in both cases.

A decomposition function $\mathcal{C} : \mathbb{C}^{m\times n} \mapsto \mathbb{R}^{2m\times n}$ and its inverse $\mathcal{C}^{-1}$ are defined as

$$\mathcal{C}(x) \triangleq \begin{bmatrix} \mathrm{Re}\{x\} \\ \mathrm{Im}\{x\} \end{bmatrix} \quad \text{and} \quad \mathcal{C}^{-1}(y) \triangleq \begin{bmatrix} I & jI \end{bmatrix} y.$$

A. Integral Quadratic Constraint

Two signals v and w are said to satisfy the IQC defined by a multiplier Π, if

$$\int_\Omega \begin{bmatrix} V(j\omega) \\ W(j\omega) \end{bmatrix}^* \Pi(j\omega) \begin{bmatrix} V(j\omega) \\ W(j\omega) \end{bmatrix} d\omega \geq 0 \tag{1}$$

where $V(j\omega)$ and $W(j\omega)$ are the Fourier transform of v and w respectively. From [17, Theorem 1], the feedback connection between H, a stable LTI system with bounded infinity norm, and a bounded causal operator $\mathbb{\Delta}$ (see Fig. 2) is stable if,

1) Interconnection of H and $\tau\mathbb{\Delta}$ is well-posed for all $\tau \in [0,1]$;
2) $\tau\mathbb{\Delta}$ satisfies the IQC defined by Π for all $\tau \in [0,1]$;
3) $\exists\, \epsilon > 0$ such that

$$\begin{bmatrix} H(j\omega) \\ I \end{bmatrix}^* \Pi(j\omega) \begin{bmatrix} H(j\omega) \\ I \end{bmatrix} \preceq -\epsilon I \qquad \forall \omega \in \Omega \tag{2}$$

Remark 1: If the upper left corner of Π is positive semi-definite and the lower right corner is negative semi-definite, then using [17, Remark 2], $\tau\mathbb{\Delta}$ satisfies the IQC defined by Π for all $\tau \in [0,1]$ if and only if $\mathbb{\Delta}$ satisfies the IQC.

Remark 2: If $\mathbb{\Delta}$ is a linear operator such that $V(j\omega) = \mathbb{\Delta}(j\omega)U(j\omega)$, then $\mathbb{\Delta}$ satisfies the IQC defined by Π, if

$$\begin{bmatrix} I \\ \mathbb{\Delta}(j\omega) \end{bmatrix}^* \Pi(j\omega) \begin{bmatrix} I \\ \mathbb{\Delta}(j\omega) \end{bmatrix} \succeq \mathbf{0} \qquad \forall \omega \in \Omega \tag{3}$$

B. Data-driven frequency-domain controller synthesis

To design a controller for a given control performance criterion, the data-driven approach presented in [18] can be used. A generalised LTI system, mapping exogenous disturbances $d \in \mathbb{R}^{n_d}$ and control inputs $u \in \mathbb{R}^{n_u}$ to performance channels $z \in \mathbb{R}^{n_z}$ and measurements $y \in \mathbb{R}^{n_y}$ is given as follows:

$$z = G_{11}d + G_{12}u$$
$$y = G_{21}d + G_{22}u$$

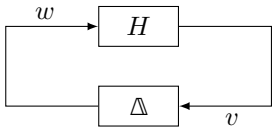

Fig. 2: Basic feedback configuration

It is assumed that only the frequency response function (FRF) of the generalised system

$$G(j\omega) = \left[\begin{array}{c:c} G_{11}(j\omega) & G_{12}(j\omega) \\ \hdashline G_{21}(j\omega) & G_{22}(j\omega) \end{array}\right] \tag{4}$$

is available, where $G_{ij}(j\omega)$ are FRFs of appropriate size. As an example, the frequency response of the discrete-time plant G_{22} can be estimated using the Fourier analysis technique from n_u sets of finite sampled input/output data, as [19]:

$$G_{22}(j\omega) = \left[\sum_{k=0}^{N-1} \mathbb{Y}(k) e^{-j\omega T_s k}\right] \left[\sum_{k=0}^{N-1} \mathbb{U}(k) e^{-j\omega T_s k}\right]^{-1} \tag{5}$$

where N is the number of data points for each experiment and T_s is the sampling period. Each column of $\mathbb{U}(k)$ and $\mathbb{Y}(k)$ represents, respectively, the inputs and outputs at the time sample k from one experiment, and n_u different experiments are needed to extract $G_{22}(j\omega)$ from the data. It is assumed that the input signal is persistently exciting. During the synthesis process, consideration can be given to the errors arising from both truncation and noise in the estimated frequency response of the plant.

The objective of the synthesis is to design a fixed-structure feedback controller K which regulates the effect of the exogenous disturbances w onto the performance channels z. The closed-loop system from w to z is given as,

$$T_{zw} = G_{11} + G_{12}K(I - G_{22}K)^{-1}G_{21}. \tag{6}$$

Under the assumption that the closed-loop system is stable, the norm of T_{zw} can be expressed using only its FRF:

$$\|T_{zw}\|_\infty^2 = \sup_{\omega\in\Omega} \overline{\sigma}\left(T_{zw}(j\omega)^* T_{zw}(j\omega)\right) \tag{7}$$

where $\overline{\sigma}(\cdot)$ is the maximum singular value and Ω the frequency spectrum. So, the minimisation of the norm can be represented as an optimisation problem,

$$\begin{aligned} &\min_{K,\,\gamma} \ \gamma \\ &\text{s.t.} \quad T_{zw}^*(j\omega)T_{zw}(j\omega) \preceq \gamma I \qquad \forall\omega\in\Omega \end{aligned} \tag{8}$$

In this paper, only the summary of the case when the left inverse of G_{12} such that $G_{12}^{\mathsf{L}}G_{12} = I$ exists $\forall\omega\in\Omega$ is given. The controller K can be structured as $K = Y^{-1}X$, where X and Y are both $\mathcal{RH}_\infty$ matrix functions that are affine with respect to the controller parameters. Denoting

$$\Phi = (Y - XG_{22})\,G_{12}^{\mathsf{L}},$$

the transfer function T_{zw} can be rewritten as

$$\begin{aligned} T_{zw} &= G_{11} + G_{12}\left(I - KG_{22}\right)^{-1} KG_{21} \\ &= G_{11} + \Phi^R X G_{21} \\ &= (\Phi^{\mathsf{R}}\Phi + \Psi)G_{11} + \Phi^{\mathsf{R}} X G_{21} \\ &= \Phi^{\mathsf{R}}\left(\Phi G_{11} + XG_{21}\right) + \Psi G_{11} \end{aligned}$$

where,

$$\Psi = I - \Phi^{\mathsf{R}}\Phi = I - G_{12}G_{12}^{\mathsf{L}},$$

So, the constraint can then be reformulated as,

$$\begin{aligned} T_{zw}^* T_{zw} = &\left(\Phi G_{11} + XG_{21}\right)^* \left(\Phi\Phi^*\right)^{-1}\left(\Phi G_{11} + XG_{21}\right) \\ &+ (\Psi G_{11})^*(\Psi G_{11}) \prec \gamma I \end{aligned} \tag{9}$$

using the fact that $\Psi^*\Phi^{\mathsf{R}} = \Psi\Phi^{\mathsf{R}} = \Phi^{\mathsf{R}} - \Phi^{\mathsf{R}}\Phi\Phi^{\mathsf{R}} = \mathbf{0}$ and $(\Phi\Phi^*)^{\mathsf{R}} = (\Phi\Phi^*)^{-1}$. Using the Schur complement lemma on (9),

$$\begin{bmatrix} \gamma I - \Lambda & \left(\Phi G_{11} + XG_{21}\right)^* \\ \left(\Phi G_{11} + XG_{21}\right) & \Phi\Phi^* \end{bmatrix} \succ \mathbf{0} \tag{10}$$

where $\Lambda = (\Psi G_{11})^*(\Psi G_{11})$. A convex lower-bound on the quadratic term $\Phi\Phi^*$ can be obtained,

$$\Phi\Phi^* \succeq \Phi\Phi_c^* + \Phi_c\Phi^* - \Phi_c\Phi_c^* \tag{11}$$

where $\Phi_c = \left(Y_c - X_cG_{22}\right)G_{12}^{\mathsf{L}}$, and $K_c = Y_c^{-1}X_c$ is an initial controller, leading to:

$$\begin{aligned} &\min_{X,\,Y,\,\Gamma} \ \gamma \\ &\begin{bmatrix} \gamma I - \Lambda & \left(\Phi G_{11} + XG_{21}\right)^* \\ \star & \Phi\Phi_c^* + \Phi_c\Phi^* - \Phi_c\Phi_c^* \end{bmatrix}(j\omega) \succ \mathbf{0} \qquad \forall\omega\in\Omega \end{aligned} \tag{12}$$

When the initial controller K_c is known to be stabilising, it can be shown using [18] that the controller K is also stabilising. For a stable plant G_{22}, a controller with a sufficiently small gain can in general stabilise the closed-loop system. In the case of an unstable plant, a stabilising controller must be available already for system identification. To solve the optimisation problem, a grid-based approach can be employed, where the controller K is used as the initial stabilising control for the next optimisation. This sequence of convex optimisation problems will converge towards a local optimal solution of the original problem due to the fact that the initial controller already satisfies the constraint and any optimisation can only improve the objective.

In cases where the number of models is small, the approach can handle multimodel uncertainty by adding constraints for each model with $\Phi^i = \left(Y - XG_{22}^i\right)G_{12}^{\mathsf{L}}$. However, when the set of models is either continuous or has a large number of models, the optimisation problem may become intractable.

C. Basic problem statement

The focus of this paper is on computing a frequency-domain uncertainty model for a MIMO system, which is consistent with data and not invalidated as defined in [20]. Furthermore, the paper also explores the application of this uncertainty model for robust data-driven control design of hybrid active-passive micro-disturbance mitigation systems.

For a MIMO plant with m input channels and n output channels, its frequency response function (FRF) matrix is the matrix where $\{k,l\}^{\text{th}}$ element is the FRF from the input channel l to the output channel k. The FRF for each measurement i is denoted using $P^i(j\omega)$. These measurements could be several independent measurements of the plant P, either at the same or different operating points or of multiple plants. The objective is to find a nominal FRF $\hat{P}$ with an uncertainty set such that it is consistent with the data.

In this paper, the aim is to minimise the impact of uncertainty on the controller performance with a 'tight' uncertainty set. The set is defined as the elementwise elliptical uncertainty around the nominal FRF of each input-output pair and 'tightness' is defined as the minimisation of the area of uncertainty at all frequencies.

For robust data-driven control design using the obtained FRF, a robustness constraint for stability has to be found. Since traditional approaches only allow disk uncertainties for each FRF, an IQC-based approach based on [16] is presented for elementwise elliptical uncertainties. Finally, this constraint would be integrated into the approach in Section II-B to find a robust controller while minimising a performance objective.

III. Main Results

The first step of the approach involves identifying the 'best' linear nominal model $\hat{P}$ and the corresponding elementwise additive elliptical uncertainty sets that are consistent with the available data. Next, this uncertainty set is transformed into an equivalent IQC formulation, which is then converted into a robust stability constraint in the frequency domain. Finally, the resulting constraint is added to the data-driven approach presented in Section II-B.

A. Optimal Additive Uncertainty Set

An optimal non-parametric additive uncertainty set represented as elementwise elliptical uncertainty is computed using tools from convex optimisation. The systems under consideration are linear time-invariant (LTI) plants represented using FRF $\{P^i(j\omega)\}$ which can be obtained from a series of m experiments using the Fourier analysis on the sampled input-output data as presented in [19].

Definition 1: A frequency response function (FRF) matrix with the elementwise additive elliptical uncertainty set can be represented as $\mathcal{M}(\hat{P}, A)(j\omega) \triangleq \hat{P}(j\omega) + \Delta$, where $\hat{P}(j\omega)$ is the nominal FRF model and Δ is the additive uncertainty set characterised by a matrix A. The element Δ_{kl} of Δ represents the additive uncertainty of $\hat{P}_{kl}(j\omega)$ from the input channel l to the output channel k and belongs to the following elliptical set:

$$\|A_{kl}(\omega)\mathcal{C}(\Delta_{kl})\|_2 \leq 1 \tag{13}$$

where, $A_{kl}(\omega) \in \mathbb{R}^{2\times 2}$ represents the ellipse parameters and $\mathcal{C}(\Delta_{kl}) \in \mathbb{R}^{2\times 1}$. The total area of the uncertainty of $\mathcal{M}(\hat{P}, A)(j\omega)$ is given as $\sum_k \sum_l \pi \det\{A_{kl}^{-1}(\omega)\}$.

It can be easily shown that a measurement $P^i(j\omega)$ belongs to $\mathcal{M}(\hat{P}, A)(j\omega)$ iff

$$\left\|A_{kl}(\omega)\mathcal{C}(P^i_{kl}(j\omega) - \hat{P}_{kl}(j\omega))\right\|_2 \leq 1 \qquad \forall k\ \forall l. \tag{14}$$

So, given the dataset $\{P^i(j\omega)\}$, a model $\mathcal{M}(\hat{P}, A)(j\omega)$ needs to be found such that

$$P^i(j\omega) \in \mathcal{M}(\hat{P}, A)(j\omega) \qquad \forall i\ \forall \omega$$

and $\mathcal{M}(\hat{P}, A)(j\omega)$ should have a minimal area of uncertainty at all frequencies for all input-output pairs. This can be defined as an optimisation problem at each frequency,

$$\min_{\hat{P},\, A} \text{ area}\, \mathcal{M}(\hat{P}, A)(j\omega) \tag{15}$$
$$\text{s.t.} \quad \left\|A_{kl}(\omega)\mathcal{C}(P^i_{kl}(j\omega) - \hat{P}_{kl}(j\omega))\right\|_2 \leq 1 \qquad \forall i\ \forall k\ \forall l$$

The objective function can be replaced by a convex function for each input-output pair such that the optimisation remains equivalent,

$$\min_{\hat{P},\, A} \text{ area}\, \mathcal{M}(\hat{P}, A)(j\omega) \Leftrightarrow \min_{\hat{P}_{kl},\, A_{kl}} \; -\log\det\{A_{kl}(\omega)\}$$

To convert the constraint into a convex constraint, a change of variable $b_{kl}(\omega) = A_{kl}(\omega)\mathcal{C}(\hat{P}_{kl}(j\omega))$ can be performed such that

$$\left\|A_{kl}(\omega)\mathcal{C}(P^i_{kl}(j\omega)) - b_{kl}(\omega)\right\|_2 \leq 1 \qquad \forall i.$$

This leads to a convex optimisation problem with a log-det objective and a conic constraint for each measurement in the dataset at all frequencies and for each input-output pair. In practical implementation, since the optimisation for controller synthesis will be performed at a finite set of frequency points Ω the following optimisation needs to be solved at these finite number of points:

$$\min_{A_{kl}, b_{kl}} \; -\log\det\{A_{kl}(\omega_n)\} \tag{16}$$
$$\text{s.t.} \quad \left\|A_{kl}(\omega_n)\mathcal{C}\left(P^i_{kl}(j\omega_n)\right) - b_{kl}(\omega_n)\right\|_2 \leq 1 \qquad \forall i$$

If we denote the optimal solutions of the above convex optimisation problem as $A^\circ_{kl}(\omega_n)$ and $b^\circ_{kl}(\omega_n)$, the best FRF $\hat{P}_{kl}(j\omega_n)$ for the elliptical uncertainty will be:

$$\hat{P}_{kl}(j\omega_n) = \mathcal{C}^{-1}\left([A^\circ_{kl}(\omega_n)]^{-1} b^\circ_{kl}(\omega_n)\right).$$

Note that, in general, the best FRF might not be any of the measured FRF of the system or their average.

Remark 3: For the matrix $A^\circ_{kl}(\omega)$ to be finite, the area of the elliptical uncertainty should be non-zero. So, there should exist at least three non-colinear points. The presence of noise, in practical scenarios, makes it improbable for this assumption to be violated.

B. Uncertainty set as IQC

In this section, the IQC multiplier Π is found such that the uncertainty of $\mathcal{M}(\hat{P}, A^\circ)$ satisfies the IQC defined by Π.

Consider a transformation matrix

$$J = \begin{bmatrix} 1 & 0 \\ 0 & j \end{bmatrix} \quad \text{with} \quad J^* J = I.$$

From the definition of $\mathcal{M}(\hat{P}, A^\circ)$, Δ_{kl} satisfies

$$\begin{aligned} &\|A^\circ_{kl}(\omega)\mathcal{C}(\Delta_{kl})\|_2 \leq 1 \qquad \forall \omega \\ \Leftrightarrow\ &\left\|A^\circ_{kl}(\omega) J^* \bar{\mathcal{C}}(\Delta_{kl})\right\|_2 \leq 1 \qquad \forall \omega \end{aligned}$$

where, $\bar{\mathcal{C}}(\Delta_{kl}) = J\mathcal{C}(\Delta_{kl})$. This can be written as,

$$\begin{bmatrix} 1 \\ \bar{\mathcal{C}}(\Delta_{kl}) \end{bmatrix}^T \begin{bmatrix} 1 & \mathbf{0} \\ \mathbf{0} & -\bar{A}^*_{kl}(j\omega)\bar{A}_{kl}(j\omega) \end{bmatrix} \begin{bmatrix} 1 \\ \bar{\mathcal{C}}(\Delta_{kl}) \end{bmatrix} \geq 0 \quad \forall \omega$$

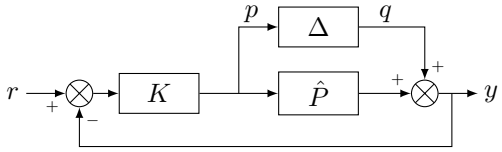

Fig. 3: Feedback system with additive uncertainty block

where $\bar{A}_{kl}(j\omega) = A^{\circ}_{kl}(\omega)J^*$. So, the uncertainty can be shown to satisfy the IQC defined by

$$\Pi_{kl}(j\omega) = \begin{bmatrix} 1 & \mathbf{0} \\ \mathbf{0} & -\bar{A}^*_{kl}(j\omega)\bar{A}_{kl}(j\omega) \end{bmatrix}. \tag{17}$$

Note that $\Pi_{kl}(j\omega)$ is a dynamic multiplier for the elliptical uncertainty set, in contrast to the frequency-dependent static gain for the disk uncertainty set. Since (17) satisfies the condition of Remark 1, $\tau\bar{\mathcal{C}}(\Delta_{kl})$ also satisfies the IQC defined by Π_{kl} for all $\tau \in [0, 1]$.

For robust controller synthesis, a single IQC for the full uncertainty block Δ is needed. By abuse of notation, denote

$$\bar{\mathcal{C}}(\Delta) = \begin{bmatrix} \mathrm{Re}\{\Delta\} \\ j\,\mathrm{Im}\{\Delta\} \end{bmatrix}.$$

It is well-known that operators with diagonal structure, in which each sub-operator meets the IQC defined by a certain multiplier, also meet the IQC defined by a structured multiplier [21]. So, the representation $\bar{\mathcal{C}}(\Delta) = L\mathcal{D}R$ where, $\mathcal{D} = \mathrm{diag}(\bar{\mathcal{C}}(\Delta_{11}), \bar{\mathcal{C}}(\Delta_{12}), \cdots, \bar{\mathcal{C}}(\Delta_{n_y n_u}))$ is desired. It can be verified that

$$L = \begin{bmatrix} I_{n_y} \otimes \mathbf{1}_{1\times n_u} \otimes \begin{bmatrix} 1 & 0 \end{bmatrix} \\ I_{n_y} \otimes \mathbf{1}_{1\times n_u} \otimes \begin{bmatrix} 0 & 1 \end{bmatrix} \end{bmatrix}, \quad \text{and} \quad R = \mathbf{1}_{n_y\times 1} \otimes I_{n_u}$$

satisfies the desired representation. Then, it can be shown that $\mathcal{D}$ satisfies the IQC defined by

$$\Pi(j\omega) = \begin{bmatrix} I & \mathbf{0} \\ \mathbf{0} & -\bar{A}^*\bar{A} \end{bmatrix}$$

where, $\bar{A} = \mathrm{diag}(\bar{A}_{11}, \ldots, \bar{A}_{kl}, \ldots, \bar{A}_{n_y n_u})$.

C. Design for Robust Stability

A robust controller K needs to be synthesised for the system $\mathcal{M}(\hat{P}, A^{\circ})$, which is graphically represented in Fig. 3. Using the data-driven approach described in Section II-B, a stabilising controller for $\hat{P}$ can be designed while minimising the performance costs. To make the controller robust, an additional robustness constraint is added at all frequency points. For the uncertainty models described by $\mathcal{M}(\hat{P}, A^{\circ})$, the uncertainty block can be split and structured as shown in Fig. 4 where $\mathcal{U}$ is the closed loop transfer function from the output to the input of the uncertainty block. Using the controller parametrization $K = Y^{-1}X$,

$$\mathcal{U} = (I + K\hat{P})^{-1}K = \phi^{-1}X$$

where, $\Phi = Y + X\hat{P}$.

The transfer function seen by $\mathcal{D}$ (see Fig. 4) is

$$H = R(\mathbf{1}_{1\times 2} \otimes -\mathcal{U})L = -R\Phi^{-1}\bar{X}L$$

with $\bar{X} = \mathbf{1}_{1\times 2} \otimes X$. Since $\mathcal{U}$ is stable by design (refer Section II-B), H is also stable. Then, using [17], if

$$\begin{bmatrix} H(j\omega) \\ I \end{bmatrix}^* \Pi \begin{bmatrix} H(j\omega) \\ I \end{bmatrix} \prec \mathbf{0} \quad \forall\omega \in \Omega \tag{18}$$

then the feedback connection between system H and $\mathcal{D}$ is stable. Using the fact that $R^*R = n_y I_{n_u}$ and

$$\begin{aligned} H^*H &= L^*\bar{X}^*\Phi^{-*}R^*R\Phi^{-1}\bar{X}L \\ &= n_y L^*\bar{X}^*\left(\Phi\Phi^*\right)^{-1}\bar{X}L, \end{aligned}$$

the inequality (18) can be written as,

$$n_y L^*\bar{X}^*\left(\Phi\Phi^*\right)^{-1}\bar{X}L - \bar{A}^*\bar{A} \prec 0.$$

Using the Schur complement lemma, an equivalent matrix inequality can be found,

$$\begin{bmatrix} \Phi\Phi^* & \bar{X}L \\ \left(\bar{X}L\right)^* & \frac{1}{n_y}\bar{A}^*\bar{A} \end{bmatrix}(j\omega) \succ \mathbf{0} \qquad \forall\omega \in \Omega. \tag{19}$$

A convex lower bound on the quadratic term $\Phi\Phi^*$ is:

$$\Phi\Phi^* \succeq \Phi\Phi_c^* + \Phi_c\Phi^* - \Phi_c\Phi_c^* \tag{20}$$

where $\Phi_c = Y_c + X_cP$, and $K_c = Y_c^{-1}X_c$ is the initial controller. This gives a sufficient condition for robust stability as a linear matrix inequality (LMI),

$$\begin{bmatrix} \Phi\Phi_c^* + \Phi_c\Phi^* - \Phi_c\Phi_c^* & \bar{X}L \\ \left(\bar{X}L\right)^* & \frac{1}{n_y}\bar{A}^*\bar{A} \end{bmatrix}(j\omega) \succ \mathbf{0} \quad \forall\omega \in \Omega \tag{21}$$

which can be added as an additional constraint in the data-driven approach presented in Section II-B.

IV. Experimental Results

A robust controller using the presented approach was designed for the hybrid active-passive micro-disturbance isolation platform presented in Section I. Due to the modular design, the FRF of the passive system stage can significantly vary depending on the applied screw torque and other mechanical system properties. The here presented method is used to design a controller which is robust with respect to variations in the torque applied to the screws holding the upper plate. A controller is designed for a configuration where the actuators are placed along the main axes having two parallel actuators per axis. In addition, three accelerometers (one along each axis) are mounted for a local measurement of the disturbances at the payload interface. The parallel nature of the actuator placement together with the three accelerometers leads to a MIMO system with three inputs and three outputs. A multimodel FRF is acquired from five different experiments with different screw torques between $6\,\mathrm{N\,m}$ and $8\,\mathrm{N\,m}$. The resulting FRFs are presented in Fig. 5. The screw torque directly influences the rigidity of the system, which can be seen by the shift in the frequency of the first mode in the interval from $45\,\mathrm{Hz}$ to $60\,\mathrm{Hz}$.

The computed elliptical uncertainty set is compared to the disk uncertainty set from [15]. From Fig. 6, it can be seen that a significant reduction of the uncertainty area can be

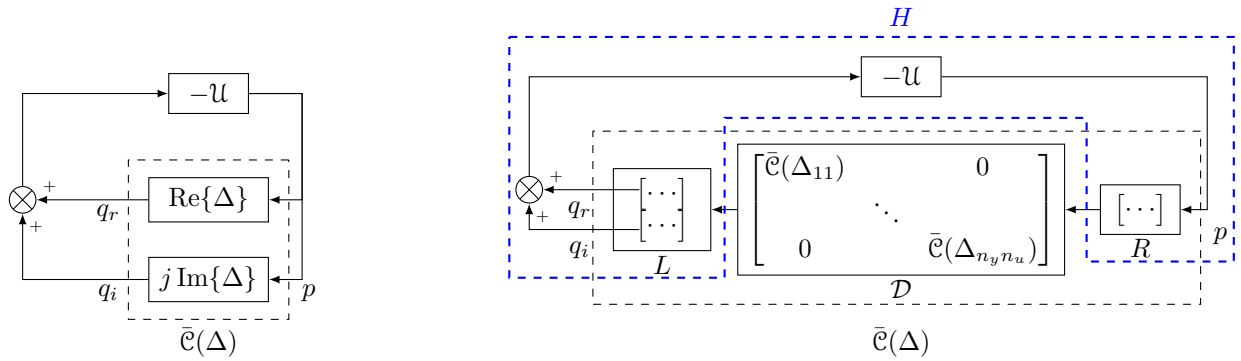

(a) Full uncertainty block

(b) Diagonalised uncertainty block

Fig. 4: Feedback system with uncertainty block split into its real and imaginary components

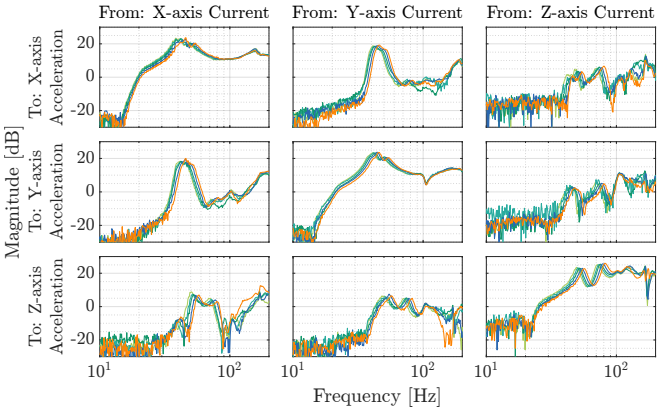

Fig. 5: Multimodel FRF from uncertain screw torque

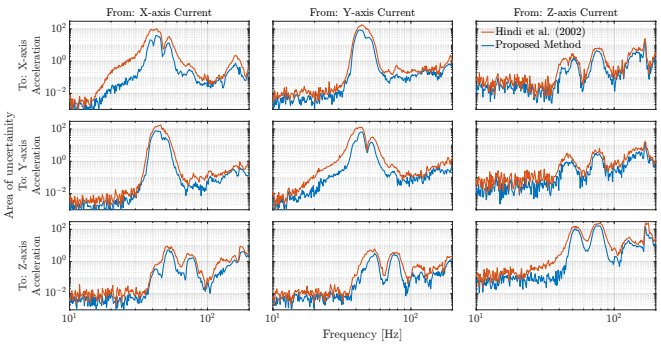

Fig. 6: Area of uncertainty model using the elliptical domains computed with the proposed method compared to circular uncertainty domains

achieved when using the elliptical uncertainty set compared to the disk uncertainty set. For the elliptical uncertainty set, the uncertainty area will always be smaller than the disk uncertainty set and in the worst-case scenario, it would be equal. A reduction factor of approximately 2.5 is observed around the frequency of the first mode.

A robust controller using the proposed method is designed for both elliptical and disk uncertainty sets. In terms of performance, the objective is the rejection of a sinusoidal perturbation at a frequency of 80 Hz. A performance objective can be added to the optimisation problem by using the following generalized system:

$$\underline{G}(j\omega) = \left[\begin{array}{c|c} W & -W\hat{P} \\ \hline I & -\hat{P} \end{array}\right](j\omega) \tag{22}$$

A performance weighting filter W is accordingly chosen as a peak filter with a centre frequency of 80 Hz. The inverse of the weighting filter along with the resulting closed-loop sensitivity functions are presented in Fig. 7. The complete optimisation problem to be solved is given by:

$$\min_{X,\,Y,\,\Gamma} \ \gamma \tag{23}$$

$$\begin{bmatrix} \gamma I - \Lambda & (\underline{\Phi}\underline{G}_{11} + X\underline{G}_{21})^* \\ \star & \underline{\Phi}\underline{\Phi}_c^* + \underline{\Phi}_c\underline{\Phi}^* - \underline{\Phi}_c\underline{\Phi}_c^* \end{bmatrix}(j\omega) \succ \mathbf{0} \qquad \forall\omega \in \Omega$$

$$\begin{bmatrix} \Phi\Phi_c^* + \Phi_c\Phi^* - \Phi_c\Phi_c^* & \bar{X}L \\ (\bar{X}L)^* & \frac{1}{n_y}\bar{A}^*\bar{A} \end{bmatrix}(j\omega) \succ \mathbf{0} \qquad \forall\omega \in \Omega,$$

where $\underline{\Phi} = (Y - X\underline{G}_{22})\,\underline{G}_{12}^{\mathsf{L}}$. From Fig. 7, one can observe that the performance objective is not attained for the disk uncertainty model because of the additional conservatism. However, the elliptical uncertainty model can ensure the desired robustness while achieving the desired performance. The computed infinity norms are 0.826 and 1.146 for the elliptical uncertainty model and disk uncertainty model respectively. When using a similar weighting filter W with a more profound notch depth, it can occur that the problem becomes infeasible using Hindi's method whereas the presented method leads to a feasible solution even if the achieved infinity norm might be larger than 1.

The designed controllers were implemented and tested on the platform for a sinusoidal perturbation at a frequency of 80 Hz injected using an external shaker along the x-axis. The achieved performance of the two controllers is presented in Fig. 8. An attenuation of 15.00 dB along the perturbed axis can be achieved compared to 10.64 dB for the controller designed with Hindi's method. The resulting attenuation performances are summarised in Table I.

V. Conclusion

Given a set of FRFs of LTI-MIMO systems, the "best" linear nominal model and the corresponding elementwise

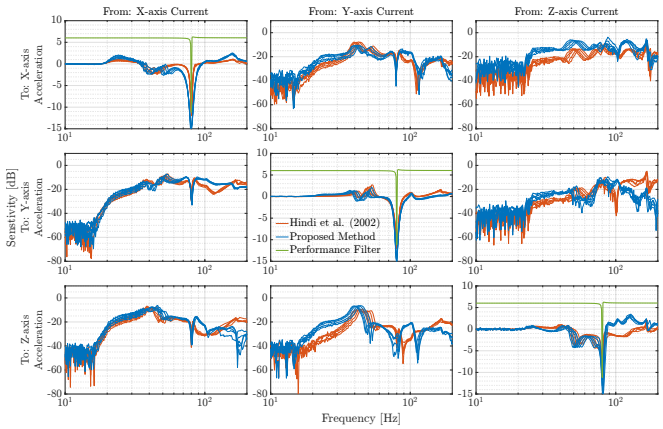

Fig. 7: Closed-loop sensitivity function comparison and performance weighting filter W^{-1}

TABLE I: Resulting attenuation performance for the two controllers along the different axes

	Attenuation Performance [dB]		
	X-axis	Y-axis	Z-axis
Proposed Method	15.00	5.60	11.93
Hindi et al. (2002)	10.64	1.74	8.39
Improvement	4.36	3.86	3.54

elliptical uncertainty set, which is consistent with the data, is found using convex optimisation. Next, the elementwise uncertainty is represented as structured diagonal uncertainty and an equivalent IQC is obtained. The resulting IQC is integrated into a data-driven frequency-domain controller synthesis method by converting it into a set of LMI constraints for robust stability. A robust controller was designed for a hybrid micro-disturbance isolation platform using the proposed method. The obtained elliptical uncertainty model showed a "tighter" uncertainty set compared to the disk uncertainty set. The experimental results demonstrated that using the elliptical uncertainty set, the area of uncertainty could be reduced up to 2.5 times and achieved an improvement of up to 4.36 dB in attenuation performance compared to the controller synthesised for the disk uncertainty set.

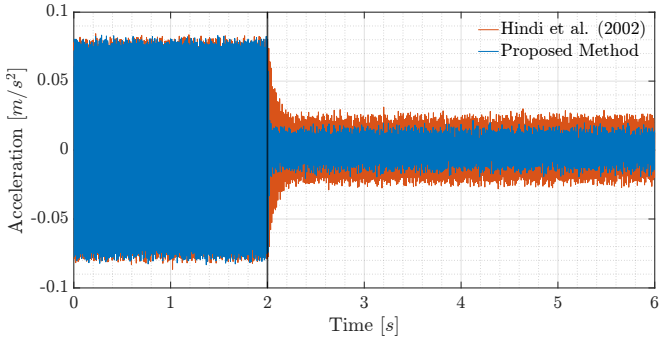

Fig. 8: Attenuation performance for the two controllers by comparison of open-loop (from 0 s to 2 s) with the closed-loop system (after 2 s)

References

[1] F. Boquet, F. Malric-Smith, and J.-P. Lejault, "Active and Passive Microvibration Mitigation System for Earth Observation and Space Science Missions," *AAS 11-064*, pp. 461–480, 2011.

[2] V. Preda, "Robust microvibration control and worst-case analysis for high pointing stability space missions," Ph.D. dissertation, Université de Bordeaux, 2017.

[3] E. Onillon, T. Adam, G. B. Gallego, and E. Klauser, "CSEM micro-vibration characterisation facility description and validation," in *European Space Mechanisms and Tribology Symposium (ESMATS)*, Warsaw, Poland, Sep. 2021.

[4] P. Apkarian and D. Noll, "Structured H_∞-control of infinite-dimensional systems," *International Journal of Robust and Nonlinear Control*, vol. 28, no. 9, pp. 3212–3238, 2018.

[5] M. Hast, K. Åström, B. Bernhardsson, and S. Boyd, "PID design by convex-concave optimization," in *2013 European Control Conference (ECC)*, Jul. 2013, pp. 4460–4465.

[6] M. Saeki, "Data-driven loop-shaping design of PID controllers for stable plants," *International Journal of Adaptive Control and Signal Processing*, vol. 28, no. 12, pp. 1325–1340, 2014.

[7] S. Boyd, M. Hast, and K. J. Åström, "MIMO PID tuning via iterated LMI restriction," *International Journal of Robust and Nonlinear Control*, vol. 26, no. 8, pp. 1718–1731, 2016.

[8] M. Saeki, M. Ogawa, and N. Wada, "Low-order H_∞ controller design on the frequency domain by partial optimization," *International Journal of Robust and Nonlinear Control*, vol. 20, no. 3, pp. 323–333, 2010.

[9] A. Karimi, A. Nicoletti, and Y. Zhu, "Robust H_∞ controller design using frequency-domain data via convex optimization," *International Journal of Robust and Nonlinear Control*, vol. 28, no. 12, pp. 3766–3783, 2018.

[10] A. Nicoletti and A. Karimi, "Robust control of systems with sector nonlinearities via convex optimization: A data-driven approach," *International Journal of Robust and Nonlinear Control*, vol. 29, no. 5, pp. 1361–1376, 2019.

[11] T. Bloemers, T. Oomen, and R. Toth, "Frequency Response Data-Driven LPV Controller Synthesis for MIMO Systems," *IEEE Control Systems Letters*, vol. 6, pp. 2264–2269, 2022.

[12] T. Bloemers, T. Oomen, and R. Tóth, "Frequency Response Data-Based LPV Controller Synthesis Applied to a Control Moment Gyroscope," *IEEE Transactions on Control Systems Technology*, vol. 30, no. 6, pp. 2734–2742, Nov. 2022.

[13] A. Karimi and C. Kammer, "A data-driven approach to robust control of multivariable systems by convex optimization," *Automatica*, vol. 85, pp. 227–233, Nov. 2017.

[14] M. G. Safonov, "Origins of Robust Control: Early History and Future Speculations," *IFAC Proceedings Volumes*, vol. 45, no. 13, pp. 1–8, Jan. 2012.

[15] H. Hindi, C.-Y. Seong, and S. Boyd, "Computing optimal uncertainty models from frequency domain data," in *Proceedings of the 41st IEEE Conference on Decision and Control*, vol. 3, Dec. 2002, pp. 2898–2905.

[16] V. Gupta, E. Klauser, and A. Karimi, "Data-driven IQC-based uncertainty modelling for robust control design," in *IFAC World Conference 2023*, Yokohama, Japan, Jul. 2023 (in press). [Online]. Available: https://infoscience.epfl.ch/record/301605

[17] A. Megretski and A. Rantzer, "System analysis via integral quadratic constraints," *IEEE Transactions on Automatic Control*, vol. 42, no. 6, pp. 819–830, Jun. 1997.

[18] P. Schuchert, V. Gupta, and A. Karimi, "Data-driven fixed-structure frequency-based $\mathcal{H}_2$ and $\mathcal{H}_\infty$ controller design," 2023 (manuscript submitted for publication). [Online]. Available: https://infoscience.epfl.ch/record/301390

[19] R. Pintelon and J. Schoukens, *System Identification: A Frequency Domain Approach*, 2nd ed. John Wiley & Sons, Ltd, 2012.

[20] M. Newlin and R. Smith, "A generalization of the structured singular value and its application to model validation," *IEEE Transactions on Automatic Control*, vol. 43, no. 7, pp. 901–907, Jul. 1998.

[21] V. M. G. B. Cavalcanti and A. M. Simões, "IQC-synthesis under structural constraints," *International Journal of Robust and Nonlinear Control*, vol. 30, no. 13, pp. 4880–4905, Sep. 2020.